Self-ordered Porous Alumina Fabricated via Phosphonic Acid Anodizing

Shunta Akiya, Tatsuya Kikuchi*,[1], Shungo Natsui, Norihito Sakaguchi, and Ryosuke O. Suzuki
Faculty of Engineering, Hokkaido University
N13-W8, Kita-ku, Sapporo, Hokkaido, 060-8628, Japan

*Corresponding author: Tatsuya Kikuchi
TEL: +81-11-706-6340
FAX: +81-11-706-6342
E-mail: kiku@eng.hokudai.ac.jp

[1] ISE active member

Abstract

Self-ordered periodic porous alumina with an undiscovered cell diameter was fabricated via electrochemical anodizing in a new electrolyte, phosphonic acid (H_3PO_3). High-purity aluminum plates were anodized in phosphonic acid solution under various operating conditions of voltage, temperature, concentration, and anodizing time. Phosphonic acid anodizing at 150-180 V caused the self-ordering behavior of porous alumina, and an ideal honeycomb nanostructure measuring 370-440 nm in cell diameter was successfully fabricated on the aluminum substrate. Conversely, disordered porous alumina grew at below 140 V, and anodizing at above 190 V caused local thickening due to oxide burning. Two-step phosphonic acid anodizing allows the fabrication of high aspect ratio ordered porous alumina. HPO_3^{2-} anions originated from the electrolyte were incorporated into the porous oxide during anodizing. Consequently, a double-layered porous alumina consisting of a thick outer layer containing incorporated HPO_3^{2-} anions, and a thin inner layer without anions was constructed via phosphonic acid anodizing.

Key words: Anodizing; Porous Alumina; Phosphonic Acid; Self-ordering; Nanostructure

1. Introduction

Porous alumina fabricated via anodizing has been widely investigated for various basic science and industrial applications such as nanostructure fabrication, electronic/optical devices, and corrosion protection [1-3]. The anodizing of aluminum and its alloys under appropriate electrochemical conditions in an appropriate electrolyte solution causes the formation of porous alumina on the aluminum surface [4]. Porous alumina possesses a nanoscale honeycomb structure with a nanopore at the center of each unit hexagonal cell, and the upper porous layer is separated from the aluminum substrate by a lower thin barrier oxide. At the end of the 1990s, the self-ordering behavior of porous alumina was reported via anodizing under optimal electrochemical conditions, including the anodizing voltage, temperature, and solution concentration, due to the rearrangement of the porous alumina during long-term anodizing [5-8]. High-aspect-ratio and highly ordered porous alumina with an ideal honeycomb structure can be easily fabricated via self-ordered anodizing and has been widely used by many researchers as a template and membrane for various nanotechnologies [13-26].

It is a well-known experimental fact that the unit cell diameter of the porous alumina (D, cell size or interpore distance) depends on the applied voltage during anodizing in aqueous electrolyte solutions under the self-ordering condition, and the relationship can be expressed by the following equation [1,27,28]

$$D = k\,U_s \qquad (1)$$

where k is a proportional constant (2.5 nm V^{-1}) and U_s corresponds to the self-ordering voltage. The self-ordering voltage is determined and limited by the electrolyte species used, and the use of several electrolytes such as sulfuric (U_s = 19-25 V) [6,7], oxalic (40 V) [7,29,30], selenic (42-48 V) [31-33], malonic (120 V) [34], phosphoric (160-195 V) [35,36], tartaric (195 V) [34], phosphonoacetic (205-225 V) [36], and etidronic acids (210-270 V) [38,39] have been reported to date through the optimum exploration for the self-ordering of porous alumina. Therefore, highly ordered porous alumina possessing a required cell diameter can be obtained by the choice of an optimal electrolyte solution and anodizing conditions. Because the self-ordering voltage and corresponding cell size are still limited to the narrow regions described above, additional electrolytes for self-ordered porous alumina must be found to expand the self-ordering voltage and cell size ranges [40].

In the present investigation, we demonstrated aluminum anodizing and its self-ordering behavior in a new electrolyte, phosphonic acid (H_3PO_3). Phosphonic acid is one of the oxoacids of phosphorus, a diacid that features two acidic hydroxyl groups with the following acid dissociation constants, pKa [41]:

$$H_3PO_3 \rightleftarrows H^+ + H_2PO_3^- \ (pKa_1 = 1.43) \qquad (1)$$

$$H_2PO_3^- \rightleftarrows H^+ + HPO_3^{2-} \ (pKa_2 = 6.54) \qquad (2)$$

Because the pKa_1 value of phosphonic acid is lower than that of phosphoric acid (H_3PO_4, pKa_1 = 1.83, pKa_2 = 6.43, pKa_3 = 11.46), it is defined as a relatively stronger acid. Empirically, the cell size of the self-ordered porous alumina showed a tendency to

decrease with the lowering of the pKa value (i.e., acid strength) [42]. Therefore, phosphonic acid anodizing may exhibit an undiscovered self-ordering voltage and corresponding cell size. Here, the self-ordering behavior of the porous alumina formed via phosphonic acid anodizing was investigated by electrochemical measurements and nanostructural observations. Consequently, highly ordered porous alumina with an additional periodicity could be successfully fabricated via two-step phosphonic acid anodizing.

2. Experimental

2.1 Pretreatment of the aluminum specimens

99.999 wt% high-purity aluminum plates (0.25-0.50 mm thick, GoodFellow, UK) were used as the starting materials for phosphonic acid anodizing. The aluminum plates were cut into 10 mm × 20 mm pieces with a handle and were then ultrasonically degreased in ethanol at room temperature for 10 min. After degreasing, the lower half of the handle of the specimens was coated with a silicon resin (KE45W, Shin-Etsu, Japan). The specimens were electropolished in a 13.6 M CH_3COOH/2.56 M $HClO_4$ (78 vol% CH_3COOH/22 vol% 70% $HClO_4$) solution at a constant cell voltage of 28 V for 1-10 min. During the electropolishing, an aluminum plate (99.99 wt%, Nippon Light Metal, Japan) was used as the cathode, and the solution was slowly stirred with a magnetic stirrer.

2.2 Phosphonic acid anodizing

The electropolished aluminum specimens were immersed in 0.5-2.0 M phosphonic acid solution (Kanto Chemical, Japan) at T = 273-293 K and were then anodized at a constant cell voltage of U = 90-190 V for t = 14 h. In the constant voltage anodizing, the following two types of anodizing were carried out: a) the voltage was applied directly to the electrodes using a direct current power supply (PWR-400H, Kikusui, Japan) connected to a PC and b) the voltage was increased linearly for the first 2.5 min and was then held at each constant voltage. A platinum plate (99.95 wt%, Nilaco, Japan) was used as the cathode for anodizing, and the solution was vigorously stirred with a cross-head stirrer bar to avoid the oxide burning phenomenon as much as possible. The current density during the constant voltage anodizing was measured by a digital multimeter (DMM4040, Tektronix, USA).

After anodizing, the specimens were immersed in a 0.2 M CrO_3/0.51 M H_3PO_4 solution at 353 K to selectively dissolve the anodic oxide. Therefore, the aluminum nanodimple array, corresponding to the negative shape of the bottom of the porous alumina, was exposed to the aluminum surface after the oxide dissolution.

2.3 Two-step phosphonic acid anodizing

For the fabrication of highly ordered porous alumina with whole vertical regions, the following two-step phosphonic acid anodizing was carried out: a) the

electropolished aluminum specimens were anodized in a 1.0 M phosphonic acid solution at 283 K and 150 V for 180 min, b) the anodic oxide was selectively dissolved in CrO_3/H_3PO_4 solution at 353 K, and c) the nanostructured specimens were anodized again under the same anodizing conditions for 15 min.

2.4 Characterization

The anodized specimens were examined by field emission scanning electron microscopy (FE-SEM, JSM-6500F and JIB-4600F/HKD, JEOL, Japan) and scanning transmission electron microscopy (STEM, Titan G2 60-300, 300 kV, FEI). For the SEM observation of the porous alumina, a thin platinum electro-conductive layer was coated onto the oxide by a platinum sputter coater (MSP-1S, Vacuum Device, Japan). For the STEM observation, the anodizing specimens were prepared by the following steps: a) highly ordered porous alumina was fabricated via two-step phosphonic acid anodizing, b) the porous alumina on one side of the specimen was selectively dissolved in 2.5 M NaOH solution to expose the aluminum substrate, and c) the specimens were immersed in 0.5 M $SnCl_4$ solution to completely dissolve the aluminum substrate. A free-standing porous alumina film without the aluminum substrate was obtained through the three steps. The porous alumina film was pasted on a molybdenum single-hole grid by an epoxy resin and was then thinned by a precision ion polishing system (PIPS, Gatan). The distribution of aluminum, oxygen, and phosphorus in the anodic oxide was examined by STEM-energy dispersive X-ray spectrometry (EDS).

3. Results and discussion

Figure 1a-1c shows the changes in the current density, j, with the anodizing time, t, at various constant voltages of U = 90-170 V in 0.5-2.0 M phosphonic acid solutions at 273 K. During the anodizing, each constant voltage was immediately applied to the electrodes from the beginning of the anodizing without any voltage increase. During anodizing at U = 140 V in 0.5 M phosphonic acid solution, the current density increased rapidly and then dropped immediately to approximately 4 Am^{-2} in the initial stage of anodizing (Fig. 1a). After this stage, the current density gradually increased again and then reached a steady value of approximately 18 Am^{-2} for 30 min. This current-time transient, including the rapid increase, rapid decrease, gradual increase, and steady state, during constant voltage anodizing is typical behavior for the formation of anodic porous alumina on the aluminum surface. The rapid increase and subsequent decrease after the voltage was applied are due to the formation of a thin anodic barrier oxide on the aluminum substrate, the gradual increase is due to the formation of pores in the barrier oxide, and the steady state current density is due to the steady growth of the porous layer [1,2,4].

As the applied voltage increased to 150 V and 160 V, the steady-state current density after the initial transition period increased with the anodizing voltage, 22 Am^{-2} at 150 V and 29 Am^{-2} at 160 V. Therefore, the growth rate of the anodic oxide may

increase with the anodizing voltage. However, the current density increased rapidly to above 40 Am^{-2} immediately after the voltage was set to 170 V, and oxygen gas was generated vigorously from the aluminum specimen. This rapid current increase with oxygen gas evolution during high voltage anodizing is known as the "oxide burning phenomenon" and is due to the ultra-high current density in localized regions caused by the high electric field applied [43-45]. A thick oxide spot with a whitish color was observed on the aluminum specimen caused by oxide burning, similar to that in phosphoric acid anodizing. Therefore, the maximum anodizing voltage for the steady growth in 0.5 M phosphonic acid solution at 273 K was determined to be U = 160 V. As the concentration of the phosphonic acid solution increased to 1.0 M and 2.0 M (Figs. 1b and 1c), the maximum anodizing voltage decreased with the concentration, 130 V in 1.0 M and 110 V in 2.0 M. To summarize, anodizing in highly concentrated phosphonic acid solution easily causes oxide burning at low applied voltages. In addition, the current density at the maximum voltage decreased considerably with the concentration of the phosphonic acid solution.

Generally, the self-ordering of the porous alumina can be achieved under the maximum voltage condition due to the highly viscous flow of the oxide under the high-current density condition. Therefore, the aluminum specimens were anodized at each maximum voltage in 0.5-2.0 M phosphonic acid solutions for the self-ordering of the porous alumina. For the observation of the self-ordering behavior of the porous alumina, the anodized specimens were immersed in CrO_3/H_3PO_4 solution to selectively dissolve the porous alumina. Therefore, a nanoscale dimple array corresponding to the bottom shape of the porous alumina (growth plane of the porous alumina) can be observed on the aluminum substrate. Figure 1d-1f shows SEM images of the exposed aluminum surface formed via phosphonic acid anodizing for 60 min and subsequent selective oxide dissolution. In 0.5 M at 160 V (Fig. 1d), numerous nanoscale dimples measuring approximately 380 nm in average diameter were formed on the aluminum surface. Although several honeycomb domains containing approximately 10 cells could be observed on the surface, the dimple array was clearly disordered over the aluminum surface under this anodizing condition. Similar disordered dimple arrays with different dimple diameters were distributed on the aluminum surface (1.0 M and 2.0 M, Figs. 1e and 1f), and the average diameter of the dimples decreased as the concentration increased. An ideal honeycomb dimple structure could not be obtained via phosphonic acid anodizing under various experimental conditions, including long-term anodizing.

In various electrolyte solutions such as phosphoric, selenic, and etidronic acids, highly ordered porous alumina with an ideal cell arrangement can be fabricated via anodizing under the maximum voltage applied, as reported previously [32,35,38]. However, phosphonic acid anodizing causes the formation of a disordered dimple array on the aluminum substrate, as described in Fig. 1. During phosphonic acid anodizing at the maximum voltages, the steady current densities were measured to be 29 Am^{-2} at 160 V in 0.5 M, 21 Am^{-2} at 130 V in 1.0 M, and 14 Am^{-2} at 110 V in 2.0 M (Figs. 1a-1c).

These current densities are significantly smaller than those in other self-ordering electrolyte solutions such as selenic and etidronic acids [32,38]. Therefore, the current density during constant voltage phosphonic acid anodizing must be increased for the self-ordering of the porous alumina. We found that a linear voltage increase in the initial stage of anodizing was required to increase the maximum voltage and the corresponding current density without oxide burning.

Figure 2a-2i shows the current-time transients at various constant voltages of U = 100-190 V in c = 0.5-2.0 M phosphonic acid solution at T = 273-293 K. In this anodizing, the voltage increased linearly for the initial 2.5 min and was then held at each constant voltage, which is different from in Fig. 1. Comparing Fig. 2a with Fig. 1a in 0.5 M phosphonic acid solution at 273 K (i.e., the same anodizing condition), the maximum voltage without oxide burning increased to 180 V from 160 V by the linear voltage sweeping in the initial stage of anodizing. Accordingly, the current density during the steady growth of the porous alumina also increased to 60 Am^{-2} from 29 Am^{-2}. A similar maximum voltage increase was also measured in 1.0 M and 2.0 M solutions (Figs. 2b and 2c). The reason why the maximum voltage increased via the linear voltage sweeping may be due to the formation of a uniform thin anodic oxide layer in the initial stage of anodizing. Lee et al. reported that a thin oxide layer should be formed on the aluminum surface before the high voltage anodizing to suppress oxide burning [28]. This oxide layer promotes uniform oxide growth without local phenomena such as a much higher current density and subsequent oxide burning. In our phosphonic acid anodizing, a similar uniform oxide layer was slowly formed during the linear voltage sweeping in the first 2.5 min of anodizing. Therefore, the subsequent maximum voltage without oxide burning may increase by using linear voltage sweeping.

As the solution temperature increased to 283 K and 293 K (Figs. 2d-2i), the maximum voltage decreased in each concentration of phosphonic acid solution. The maximum voltage also decreased with the solution concentration at each temperature of the solution. Figure 3 summarizes the maximum voltage, U_{max}, and temperature, T, in different solution concentrations, c, obtained for linear sweep phosphonic acid anodizing. The maximum voltage decreases linearly with the temperature increase in each concentration. High concentration and temperature induce the chemical dissolution of the barrier oxide at the bottom of the porous layer due to the high chemical solubility of the phosphonic acid solution. Therefore, the maximum voltage for the steady growth without oxide burning decreases with the solution concentration and temperature. This tendency is typically observed in other electrolyte solutions [32]. In other words, the wide maximum voltage regions between 110 V and 180 V during phosphonic acid anodizing could be accurately achieved by the selection of an optimum concentration and temperature. This selectivity of the maximum voltage is an important result for the fabrication of ordered porous alumina with different cell diameters, as described later. The regularity of the dimple array formed by linear voltage sweeping was observed by SEM.

Figure 4 shows SEM images of the typical aluminum surface obtained via anodizing in 0.5-2.0 M phosphonic acid solutions (T = 273-293 K) at each corresponding maximum voltage for 60 min processing with subsequent selective oxide dissolution. Comparing linear voltage sweeping with direct voltage application (Fig. 1), relatively large honeycomb domains with several tens of dimples were observed on the aluminum surface in most cases because the porous layer was self-ordered by rapid oxide growth at high current density under the improved maximum voltage anodizing. Conversely, it was observed that the dimple array was disordered at the lowest voltage of 110 V. It is observed from Fig. 4 that the average diameter of the dimples decreases with the applied voltage.

Figure 5a-5c shows SEM images of the surface of the porous oxide formed via anodizing in a 2.0 M phosphonic acid solution at 273-293 K under the maximum voltage applied, as described in Figs. 4c, 4f, and 4i. At a temperature of 273 K (Fig. 5a), numerous nanopores measuring several tens of nanometers in diameter can be observed on the anodic oxide. In typical porous oxide growth, the nanopores are generated in a disorderly fashion in the barrier oxide during the initial stage of anodizing, and then nanopores with an equal interval corresponding to the applied voltage grow via the long-term anodizing due to their rearrangement. Therefore, many mature nanopores with a black color (i.e., deep nanopores) and also numerous extinct nanopores with a gray color (i.e., shallow nanopores) were located together on the surface of the porous alumina. The diameter of these nanopores increased with the temperature of phosphonic acid solution (Figs. 5b and 5c) because the top part of the porous alumina formed in the initial stage of anodizing was chemically dissolved at high temperatures. This chemical dissolution of the porous alumina is typically observed in long-term anodizing in other strong acid solutions [46]. Therefore, it is important to consider such chemical dissolution behaviors for the fabrication of highly ordered porous alumina via a) long-term, b) high-temperature, and c) high-concentration phosphonic acid anodizing.

From previous experimental knowledge, it is known that long-term anodizing is an effective approach for the self-ordering of porous alumina [5]. Therefore, we demonstrated long-term phosphonic acid anodizing under several selected experimental conditions. Figure 6 shows a current density-time transient during long-term anodizing in a 0.5 M phosphonic acid solution at 180 V and 273 K for 14 h (840 min). After the initial transition period of anodizing, the current density increased to approximately 55 Am^{-2} for 15 min, the same as in Fig. 2a. The current density then gradually increased during the long-term anodizing and exhibited a large value of approximately 90 Am^{-2} after 14-h-anodizing. Such gradual current increases during the long-term constant voltage anodizing were also measured under different anodizing conditions. Figure 7 shows SEM images of dimple arrays fabricated on the aluminum substrate via phosphonic acid anodizing in a) 0.5 M at 180 V and 273 K for 14 h, b) 0.5 M at 160 V and 283 K for 8 h, and c) 1.0 M at 150 V and 283 K for 3 h. Ideal dimple arrangements with more than one hundred dimples measuring a) 440 nm at 180 V, b) 382 nm at 160 V,

and c) 372 nm at 150 V in dimple diameter were successfully fabricated via long-term phosphonic acid anodizing under each operating condition. These diameter-voltage values are consistent with the linear relations obtained via self-ordering anodizing in other electrolyte solutions, as described in Equation 1.

For the further extension of the self-ordering voltage via phosphonic acid anodizing, an electropolished specimen was anodized in 0.5 M at a lower voltage of 140 V and 293 K, as shown in Fig. 8a. After the initial stage of anodizing, the current density exhibited a relatively high value of approximately 200 Am^{-2} for up to 4 h. However, the current density then increased rapidly to above 500 Am^{-2}, and non-uniform anodic oxide was formed on the aluminum specimen due to oxide burning. Because excess anodizing in the phosphonic acid solution caused such oxide burning, long-term anodizing should be stopped at an appropriate time before oxide burning occurs under each operating condition. Figure 8b shows an SEM image of the exposed aluminum surface obtained via phosphonic acid anodizing under same operating conditions for 4 h before oxide burning. Although a small honeycomb domain consisting of several dimples can be observed on the aluminum surface, a disordered dimple array with many different cell diameters and white defects at the apices of the dimple structure were formed under this condition. Similarly, low-voltage phosphonic acid anodizing at below 150 V under other operating conditions causes the formation of a disordered dimple array on the aluminum surface. Through the experimental results in Figs. 2-8, the self-ordering region of phosphonic acid anodizing could be summarized to be 370-440 nm at 150-180 V. Figure 9 summarizes the self-ordering voltage, U_s, and the obtained cell size, D, during aluminum anodizing in various electrolyte solutions, including phosphonic acid. As described in the introduction, phosphoric acid anodizing at 160-195 V allows the fabrication of self-ordered porous alumina measuring 405-500 nm in cell diameter [1]. Although the self-ordering regions of phosphoric and phosphonic acid anodizing overlap in the range of 160 to 180 V, our phosphonic acid anodizing further expands the previously unutilized self-ordering voltage of 150-160 V. Therefore, phosphonic acid anodizing is a useful process for the fabrication of ordered nanostructures with 370-400 nm periodicity. It should be noted that this self-ordering region could only be achieved via phosphonic acid anodizing. Because the self-ordering region corresponds to the ultraviolet (UV) wavelength, the fabricated nanostructures may exhibit unique optical properties such as UV selective reflection [32, 33].

For the fabrication of high-aspect-ratio and highly ordered porous alumina, two-step phosphonic acid anodizing was demonstrated as follows: a) the first self-ordering anodizing in 1.0 M phosphonic acid at 150 V and 283 K for 3 h, b) the selective oxide dissolution in CrO_3/H_3PO_4 solution, and c) the second self-ordering anodizing in 1.0 M phosphonic acid at 150 V and 283 K for 15 min. Figure 10a shows an SEM image of the fracture vertical cross-section of the self-ordered porous alumina fabricated via two-step phosphonic acid anodizing. Here, the top white, middle gray, and bottom gray regions correspond to the oxide surface, porous layer, and aluminum

substrate, respectively. A high-aspect-ratio ordered porous alumina was successfully formed on the aluminum substrate via two-step phosphonic acid anodizing, and parallel cylindrical nanopores without any defects such as an intercrossing structure can be observed in the porous layer. A high-magnification SEM image of the porous layer is shown in Fig. 10b, and the pore diameter of the porous alumina fabricated in this anodizing condition was measured to be 132 nm. The pore diameter of the porous alumina can be further expanded by long-term immersion in appropriate acidic solutions after the anodizing (i.e., pore-widening) [46]. Figure 10c shows an SEM image of the fracture transverse plane of the porous alumina. Each circular nanopore was distributed hexagonally within the anodic oxide (however, cell boundaries cannot be observed here), and the arrangement periods were measured to be 374 nm. This value agrees with the value measure on the aluminum nanodimple array. As described in Fig. 10, two-step phosphonic acid anodizing allows the fabrication of highly ordered porous alumina with high-aspect-ratio nanopores. Such an ordered nanostructure can be applied to various nanotemplate and membrane technologies.

The highly ordered porous alumina fabricated via two-step phosphonic acid anodizing was physically thinned by an ion beam for SEM and STEM observations. Figure 11a shows an SEM image of the ordered porous alumina in a large region. Nano-scale pores were regularly distributed over the wide area of the thinning oxide plane, although non-circular pores were slightly observed. For the fabrication of the ideal porous alumina, it may be useful to combine imprinting techniques with self-ordered anodizing. Figure 11b-11e shows high-angle annular dark field (HAADF)-STEM images and the aluminum, oxygen, and phosphorus element distributions obtained by EDS analysis of the ordered porous alumina. White hexagonal cell boundaries measuring approximately 45 nm in width were clearly observed in the HAADF-STEM images (Fig. 11b). The aluminum element was distributed over the whole region of the oxide, but the aluminum concentration at the cell boundaries corresponding to the inner oxide layer was slightly higher than that in the outer oxide layer (Fig. 11c). In the phosphorus distribution, phosphorus-free cell boundaries with a honeycomb configuration were clearly measured (Fig. 11e). Conversely, the oxygen element was uniformly distributed in the anodic oxide (Fig. 11d). To summarize, the elemental mapping images indicate that the anodic oxide formed via phosphonic acid anodizing consists of the outer alumina layer with phosphorous anions and the inner pure alumina layer.

Porous alumina fabricated via anodizing in three major electrolyte solutions, i.e., sulfuric, oxalic, and phosphoric acid, typically consists of amorphous aluminum oxide containing a small amount of anions of the electrolyte used [1,4]. The acid anions are incorporated into the oxide via inward migration under an electric field during anodizing. The distribution of the anions in the oxide depends on the electrolyte solution, and the thickness of the outer oxide containing anions incorporated from the electrolyte solution increases in the order of a) sulfuric, b) oxalic, and c) phosphoric

acids. For example, porous alumina fabricated via phosphoric acid anodizing consists of a) a thick outer oxide layer containing incorporated phosphorus anions and b) a thin inner oxide layer without anions [47]. In the case of our phosphonic acid anodizing, the elemental distribution behaviors are in fair agreement with those of phosphoric acid anodizing. Therefore, it is considered that HPO_3^{2-} anions are incorporated into the oxide during phosphonic acid anodizing through the same incorporation behavior exhibited during phosphoric acid anodizing. On the other hand, it was reported that there was an interstitial rod with a different composition at the triple point of the hexagonal cells in the porous alumina fabricated via phosphoric acid anodizing [47]. However, such a rod-like nanostructure could not be observed in the porous alumina fabricated via phosphonic acid anodizing (Fig. 11b).

4. Conclusions

A novel anodizing electrolyte for producing self-ordered porous alumina, phosphonic acid, was demonstrated under various electrochemical anodizing conditions. We found that phosphonic acid anodizing creates highly ordered porous alumina with a cell diameter measuring 370-440 nm via self-ordering conditions at 150-180 V. Importantly, the previously undiscovered self-ordering voltage of 150 V was achieved via phosphonic acid anodizing. Conversely, phosphonic acid anodizing at below 140 V and above 190 V causes the formation of unordered porous alumina and oxide burning, respectively. High-aspect-ratio self-ordered porous alumina can be easily fabricated via two-step phosphonic acid anodizing. HPO_3^{2-} anions are incorporated into the anodic oxide by a high electric field during anodizing, and a double-layered porous alumina with an outer alumina layer with anions and an inner pure alumina layer is formed via phosphonic acid anodizing.

Acknowledgments

This study was conducted at Hokkaido University and was supported by the "Nanotechnology Platform" Program of the Ministry of Education, Culture, Sports, Science, and Technology (MEXT), Japan. The authors would like to thank Mr. Nobuyuki Miyazaki, Mr. Takashi Endo, and Mr. Ryo Oota for their assistance in the SEM and STEM observations. This study was financially supported by the Light Metal Educational Foundation and The Sumitomo Foundation (No. 151181), Japan.

References

1) W. Lee, S.-J. Park, Porous anodic aluminum oxide: anodization and templated synthesis of functional nanostructures, Chemical Reviews 114 (2014) 7487.
2) G.D. Sulka, Highly ordered anodic porous alumina formation by self-organized anodizing, in: A. Eftekhari (Ed.), Nanostructured Materials in Electrochemistry, Wiley-VCH, 2008, p. 1.
3) F. Mansfeld, M.W. Kendig, Evaluation of anodized aluminum surfaces with

electrochemical impedance spectroscopy, Journal of The Electrochemical Society 135 (1988) 828.
4) G.E. Thompson, Porous anodic alumina: fabrication, characterization and applications, Thin Solid Films 297 (1997) 192.
5) H. Masuda, K. Fukuda, Ordered metal nanohole arrays made by a two-step replication of honeycomb structures of anodic alumina, Science 268 (1995) 1466.
6) H. Masuda, F. Hasegwa, S. Ono, Self-ordering of cell arrangement of anodic porous alumina formed in sulfuric acid anodizing, Journal of The Electrochemical Society 144 (1997) L127.
7) A.P. Li, F. Müller, A. Birner, K. Nielsch, U. Gösele, Hexagonal pore arrays with a 50–420 nm interpore distance formed by self-organization in anodic alumina, Journal of Applied Physics, 84 (1998) 6023.
8) O. Jessensky, F. Müller, U. Gösele, Self-organized formation of hexagonal pore arrays in anodic alumina, Applied Physics Letters 72 (1998) 1173.
9) M. Michalska-Domańska, M. Norek, W.J. Stępniowski, B. Budner, Fabrication of high quality anodic aluminum oxide (AAO) on low purity aluminum—A comparative study with the AAO produced on high purity aluminum, Electrochimica Acta 105 (2013) 424.
10) L. Zaraska, W.J. Stępniowski, G.D. Sulka, E. Ciepiela, M. Jaskuła, Analysis of nanopore arrangement and structural features of anodic alumina layers formed by two-step anodizing in oxalic acid using the dedicated executable software, Applied Physics A 114 (2014) 571.
11) W.J. Stępniowski, A. Nowak-Stępniowska, A. Presz, T. Czujko, R.A. Varin, The effects of time and temperature on the arrangement of anodic aluminum oxide nanopores, Materials characterization 91 (2014) 1.
12) G.D. Sulka, A. Brzózka, L. Zaraska, M. Jaskuła, Through-hole membranes of nanoporous alumina formed by anodizing in oxalic acid and their applications in fabrication of nanowire arrays, Electrochimica Acta 55 (2010) 4368.
13) T. Yanagishita, H. Masuda, Carbon nanofiber arrays from high-aspect ratio polymer pillar prepared by nanoimprinting using anodic porous alumina, Materials Letters 160 (2015) 235.
14) T. Kondo, N. Kitagishi, T. Yanagishita, H. Masuda, Surface-enhanced Raman scattering on gold nanowire array formed by mechanical deformation using anodic porous alumina molds, Applied Physics Express 8 (2015) 062002.
15) T. Ozel, G.R. Bourret, C.A. Mirkin, Coaxial lithography, Nature Nanotechnology 10 (2015) 319.
16) A. Al-Haddad, Z. Zhan, C. Wang, S. Tarish, R. Vellacheria, Y. Lei, Facile transferring of wafer-scale ultrathin alumina membranes onto substrates for nanostructure patterning, ACS Nano 9 (2015) 8584.
17) T. Yanagishita, Y. Maejima, K. Nishio, H. Masuda, Monodisperse nanoparticles of metal oxides prepared by membrane emulsification using ordered anodic porous

alumina, RSC Advances 4 (2014) 1538.
18) K. Kant, C. Priest, J.G. Shapter, D. Losic, Characterization of impedance biosensing performance of single and nanopore arrays of anodic porous alumina fabricated by focused ion beam (FIB) milling, Electrochimica Acta 139 (2014) 225.
19) W. Lee, K. Schwirn, M. Steinhart, E. Pippel, R. Schols, U. Gösele, Structural engineering of nanoporous anodic aluminium oxide by pulse anodization of aluminium, Nature Nanotechnology 3 (2008) 234.
20) J. Yao, Z. Liu, Y. Liu, Y. Wang, C. Sun, G. Bartal, A.M. Stacy, X. Zhang, Optical negative refraction in bulk metamaterials of nanowires, Science 321 (2008) 930.
21) J. Martín, M. Martín-González, J.F. Fernández, O. Caballero-Calero, Ordered three-dimensional interconnected nanoarchitectures in anodic porous alumina, Nature Communications 5 (2014) 5130.
22) D. Liu, C. Zhang, G. Wang, Z. Shao, X. Zhu, N. Wang, H. Cheng, Nanoscale electrochemical metallization memories based on amorphous (La, Sr) MnO_3 using ultrathin porous alumina masks, Journal of Physics D: Applied Physics (2014) 085108.
23) L. Wang, X. Qin, D. Ji, J.P. Parry, J. Zhang, C. Deng, G. Ding, Q. Gan, H. Zeng, X. Xu, Engineering optical properties of metal/porous anodic alumina films for refractometric sensing, Applied Surface Science 355 (2015) 139.
24) W.J. Stępniowski, W. Florkiewicz, M. Michalska-Domańska, M. Norek, T. Czujko, A comparative study of electrochemical barrier layer thinning for anodic aluminum oxide grown on technical purity aluminum, Journal of Electroanalytical Chemistry 741 (2015) 80.
25) E. Pechkova, N.L. Bragazzi, C. Nicolini, Protein Crystallization by Anodic Porous Alumina (APA) Template: The Example of Hen Egg White Lysozyme (HEWL), NanoWorld Journal 1 (2015) 46
26) M. Aramesh, W. Tong, K. Fox, A. Turnley, D.H. Seo, S. Prawer, K.K. Ostrikov, Nanocarbon-coated porous anodic alumina for bionic devices, Materials 8 (2015) 4992.
27) S.Z. Chu, K. Wada, S. Inoue, M. Isogai, Y. Katsuta, A. Yasumori, Large-scale fabrication of ordered nanoporous alumina films with arbitrary pore intervals by critical-potential anodization, Journal of The Electrochemical Society 153 (2006) B384.
28) W. Lee, R. Ji, U. Gösele, K. Nielsch, Fast fabrication of long-range ordered porous alumina membranes by hard anodization, Nature Materials 5 (2006) 741.
29) O. Jessensky, F. Müller, U. Gösele, Self-organized formation of hexagonal pore arrays in anodic alumina, Applied Physics Letters 72 (1998) 1173.
30) L. Zaraska, W.J. Stępniowski, M. Jaskuła, G.D. Sulka, Analysis of nanopore arrangement of porous alumina layers formed by anodizing in oxalic acid at relatively high temperatures, Applied Surface Science 305 (2014) 650.
31) O. Nishinaga, T. Kikuchi, S. Natsui, R.O. Suzuki, Rapid fabrication of self-ordered

porous alumina with 10-/sub-10-nm-scale nanostructures by selenic acid anodizing, Scientific reports 3 (2013) 2748.
32) T. Kikuchi, O. Nishinaga, S. Natsui, R.O. Suzuki, Self-ordering behavior of anodic porous alumina via selenic acid anodizing, Electrochimica Acta 137 (2014) 728.
33) S. Akiya, T. Kikuchi, S. Natsui, R.O. Suzuki, Optimum exploration for the self-ordering of anodic porous alumina formed via selenic acid anodizing, Journal of The Electrochemical Society 162 (2015) E244.
34) S. Ono, M. Saito, H. Asoh, Self-ordering of anodic porous alumina formed in organic acid electrolytes, Electrochimica Acta 51 (2005) 827.
35) H. Masuda, K. Yada, A. Osaka, Self-ordering of cell configuration of anodic porous alumina with large-size pores in phosphoric acid solution, Japanese Journal of Applied Physics 37 (1998) L1340.
36) K. Nielsch, J. Choi, K. Schwirn, R.B. Wehrspohn, U. Gösele, Self-ordering regimes of porous alumina: The 10% porosity rule, Nano Letters 2 (2002) 677.
37) A. Takenaga, T.Kikuchi, S. Natsui, R.O. Suzuki, Self-ordered aluminum anodizing in phosphonoacetic acid and its structural coloration, ECS Solid State Letters 4 (2015) P55.
38) T. Kikuchi, O. Nishinaga, S. Natsui, R.O. Suzuki, Fabrication of self-ordered porous alumina via etidronic acid anodizing and structural color generation from submicrometer-scale dimple array, Electrochimica Acta 156 (2015) 235.
39) T. Kikuchi, O. Nishinaga, S. Natsui, R.O. Suzuki, Polymer nanoimprinting using an anodized aluminum mold for structural coloration, Applied Surface Science 341 (2015) 19.
40) T. Kikuchi, D. Nakajima, O. Nishinaga, S. Natsui, R.O. Suzuki, Porous aluminum oxide formed by anodizing in various electrolyte species, Current Nanoscience 11 (2015) 560.
41) Y. Iwasawa, Handbook of Chemistry, Pure chemistry-II, fifth ed., Maruzen, Tokyo, 2004. P. 333.
42) D. Nakajima, T. Kikuchi, S. Natsui, R.O. Suzuki, Growth behavior of anodic oxide formed by aluminum anodizing in glutaric and its derivative acid electrolytes, Applied Surface Science 321 (2014) 364.
43) T. Aerts, I. De Graeve, H. Terryn, Study of initiation and development of local burning phenomena during anodizing of aluminium under controlled convection, Electrochimica Acta 54 (2008) 270.
44) T. Aerts, I. De Graeve, H. Terryn, Anodizing of aluminium under applied electrode temperature: Process evaluation and elimination of burning at high current densities, Surface and Coatings Technology 204 (2010) 2754.
45) S. Ono, M. Saito, H. Asoh, Self-ordering of anodic porous alumina induced by local current concentration: Burning, Electrochemical and Solid-State Letters 7 (2004) B21.
46) M. Nagayama, K. Tamura, H. Takahashi, Mechanism of open-circuit dissolution of

porous oxide films on aluminium in acid solutions, Corrosion Science 12 (1972) 133.
47) F. Le Coz, L. Arurault, L. Datas, Chemical analysis of a single basic cell of porous anodic aluminium oxide templates, Materials Characterization 61 (2010) 283.

Captions

Figure 1. a)-c) Changes in the current density, j, at time, t, during anodizing in 0.5-2.0 M phosphonic acid solution at 273 K and different applied voltages. The maximum voltage without oxide burning was determined by these electrochemical measurements. d)-f) SEM images of the nanostructured aluminum surface fabricated via phosphonic acid anodizing at the maximum voltage for 60 min. After anodizing, the anodic oxide was selectively dissolved in CrO_3/H_3PO_4 solution, and the aluminum dimple array was exposed to the surface.

Figure 2. Changes in the current density, j, at time, t, during phosphonic acid anodizing under various concentrations (c = 0.5-2.0 M), temperatures (T = 273-293 K), and voltages (U = 100-190 V). In this anodizing, the voltage increased linearly for the first 2.5 min and then was held at constant voltage to avoid oxide burning, which is different from Fig. 1.

Figure 3. Effects of temperature, T, on the maximum voltage, U_{max}, for anodizing in 0.5-2.0 M phosphonic acid solution.

Figure 4. SEM images of the nanostructured aluminum surface fabricated via phosphonic acid anodizing for 60 min under maximum voltage conditions, as described in Fig. 3.

Figure 5. SEM images of the surface of the porous alumina formed by anodizing in 2.0 M phosphonic acid solution at different temperatures (273-293 K) and anodizing voltages (110-160 V).

Figure 6. Change in the current density, j, at time, t, during long-term anodizing in 0.5 M phosphonic acid solution at 180 V and 273 K for 14 h.

Figure 7. SEM images of the ordered dimple array fabricated on the aluminum surface after phosphonic acid anodizing under the following conditions: a) 0.5 M at 180 V and 273 K for 14 h, b) 0.5 M at 160 V and 283 K for 8 h, and c) 1.0 M at 150 V and 283 K for 3 h.

Figure 8. a) Change in the current density, j, at time, t, during anodizing in 0.5 M phosphonic acid solution at 140 V and 293 K. b) An SEM image of the dimple array fabricated on the aluminum surface after phosphonic acid anodizing under the same operating conditions for 4 h before oxide burning.

Figure 9. Linear relationship of the self-ordering voltage, U_s, and the cell size, D, for

self-ordered porous alumina obtained via aluminum anodizing in various electrolyte solutions including sulfuric, oxalic, selenic, malonic, phosphoric, tartaric, phosphonoacetic, etidronic, and phosphonic acids.

Figure 10. SEM images of the fracture cross-section of the highly ordered porous alumina fabricated via two-step phosphonic acid anodizing at a self-ordering voltage of 150 V.

Figure 11. a) SEM, b) HAADF-STEM, and c)-e) elemental distribution mapping images of aluminum, oxygen, and phosphorus in the porous alumina fabricated via phosphonic acid anodizing at 150 V.

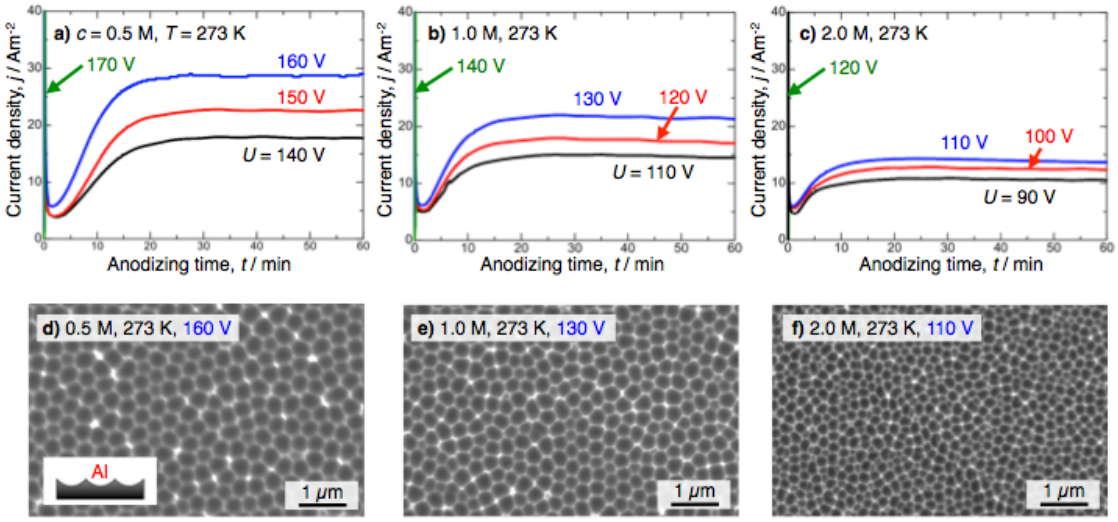
a) c = 0.5 M, T = 273 K
170 V
160 V
150 V
U = 140 V
Current density, j / Am-2
Anodizing time, t / min
b) 1.0 M, 273 K
140 V
130 V
120 V
U = 110 V
Current density, j / Am-2
Anodizing time, t / min
c) 2.0 M, 273 K
120 V
110 V
100 V
U = 90 V
Current density, j / Am-2
Anodizing time, t / min
d) 0.5 M, 273 K, 160 V
Al
1 μm
e) 1.0 M, 273 K, 130 V
1 μm
f) 2.0 M, 273 K, 110 V
1 μm

Figure 1.

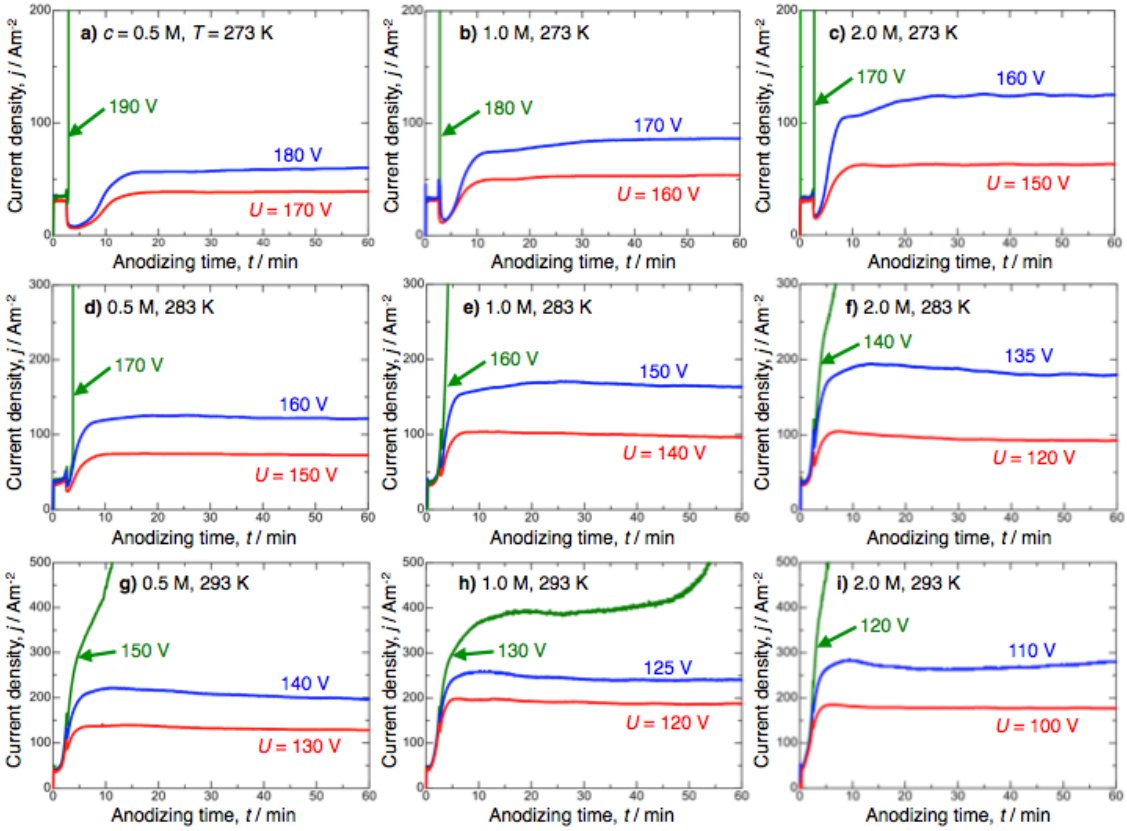
a) c = 0.5 M, T = 273 K
190 V
180 V
U = 170 V
b) 1.0 M, 273 K
180 V
170 V
U = 160 V
c) 2.0 M, 273 K
170 V
160 V
U = 150 V
d) 0.5 M, 283 K
170 V
160 V
U = 150 V
e) 1.0 M, 283 K
160 V
150 V
U = 140 V
f) 2.0 M, 283 K
140 V
135 V
U = 120 V
g) 0.5 M, 293 K
150 V
140 V
U = 130 V
h) 1.0 M, 293 K
130 V
125 V
U = 120 V
i) 2.0 M, 293 K
120 V
110 V
U = 100 V
Current density, j / Am-2
Anodizing time, t / min

Figure 2.

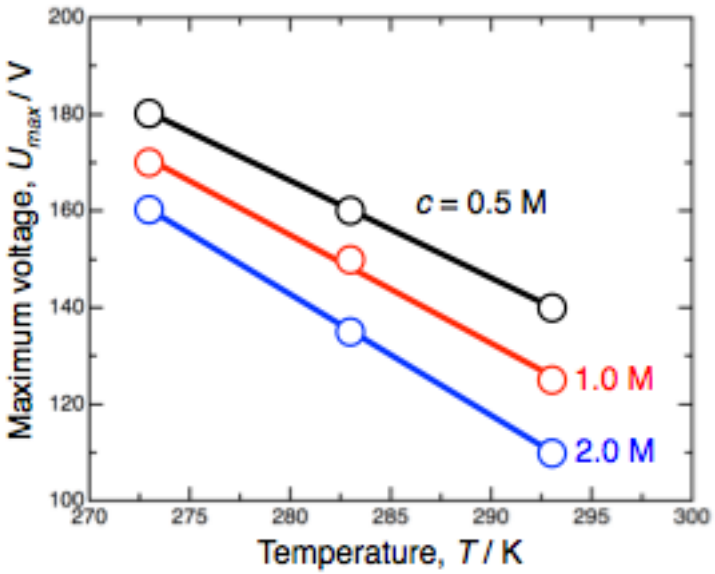
Maximum voltage, U_{max} / V
200
180
160
140
120
100
270
275
280
285
290
295
300
Temperature, T / K
c = 0.5 M
1.0 M
2.0 M

Figure 3.

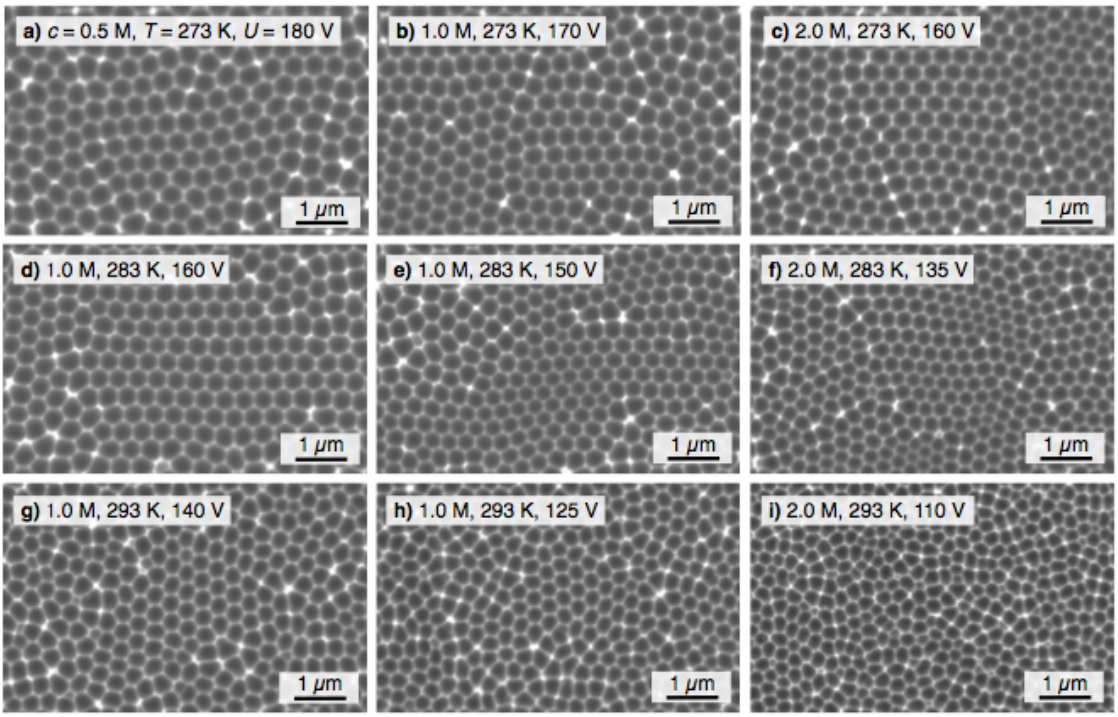
a) c = 0.5 M, T = 273 K, U = 180 V
b) 1.0 M, 273 K, 170 V
c) 2.0 M, 273 K, 160 V
d) 1.0 M, 283 K, 160 V
e) 1.0 M, 283 K, 150 V
f) 2.0 M, 283 K, 135 V
g) 1.0 M, 293 K, 140 V
h) 1.0 M, 293 K, 125 V
i) 2.0 M, 293 K, 110 V
1 μm

Figure 4.

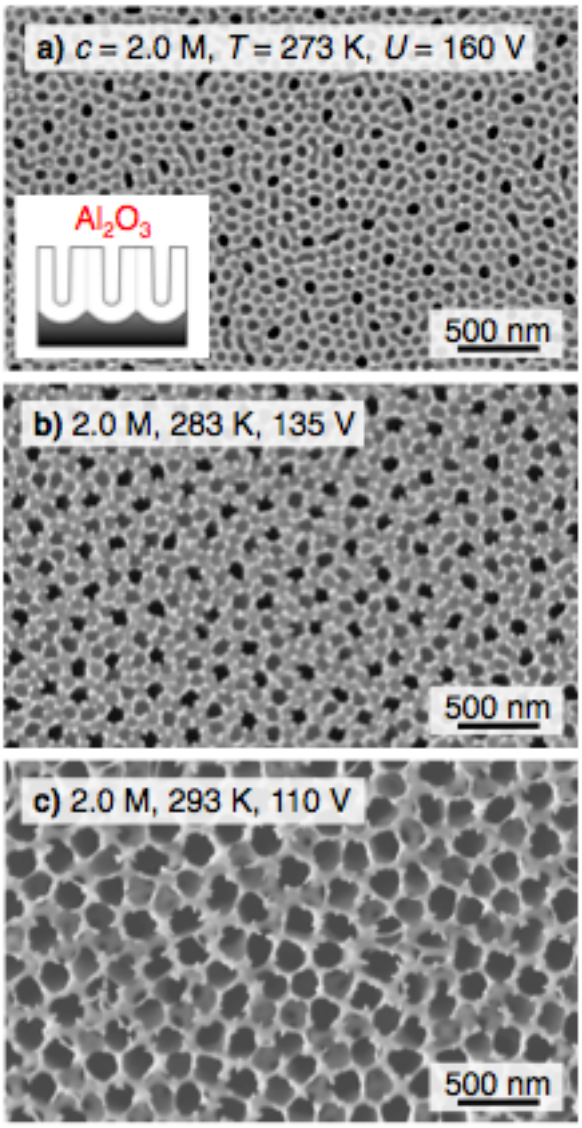
a) c = 2.0 M, T = 273 K, U = 160 V
Al2O3
500 nm
b) 2.0 M, 283 K, 135 V
500 nm
c) 2.0 M, 293 K, 110 V
500 nm

Figure 5.

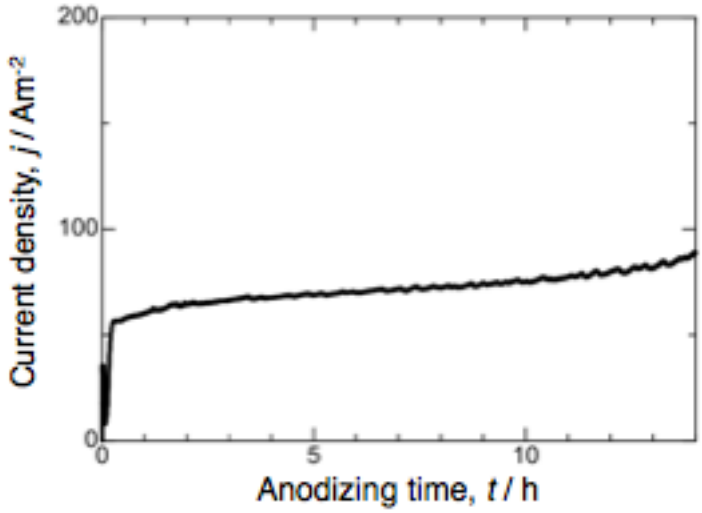

Figure 6.

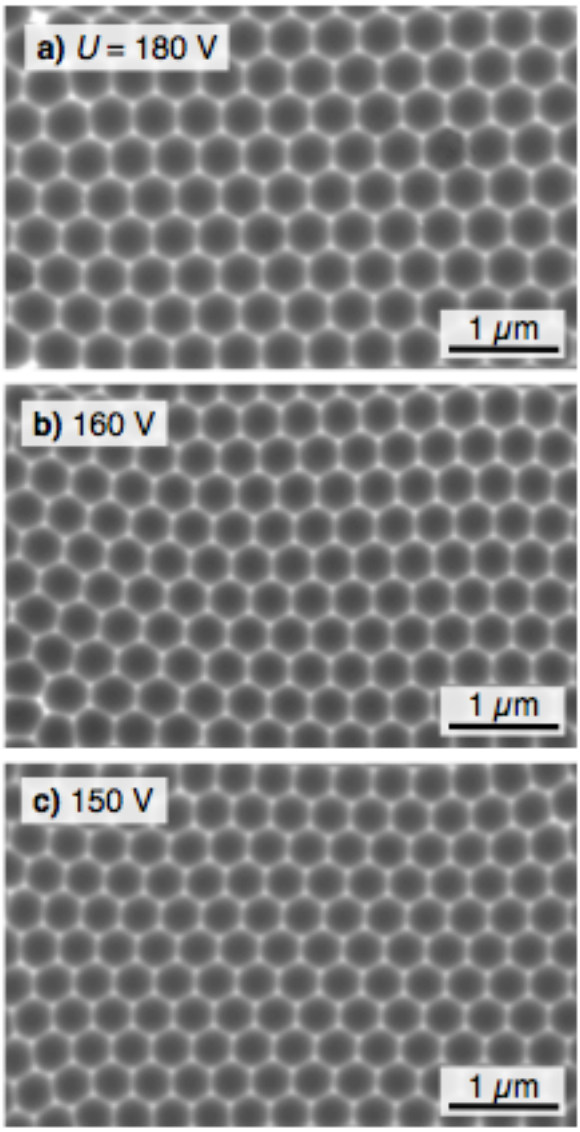

Figure 7.

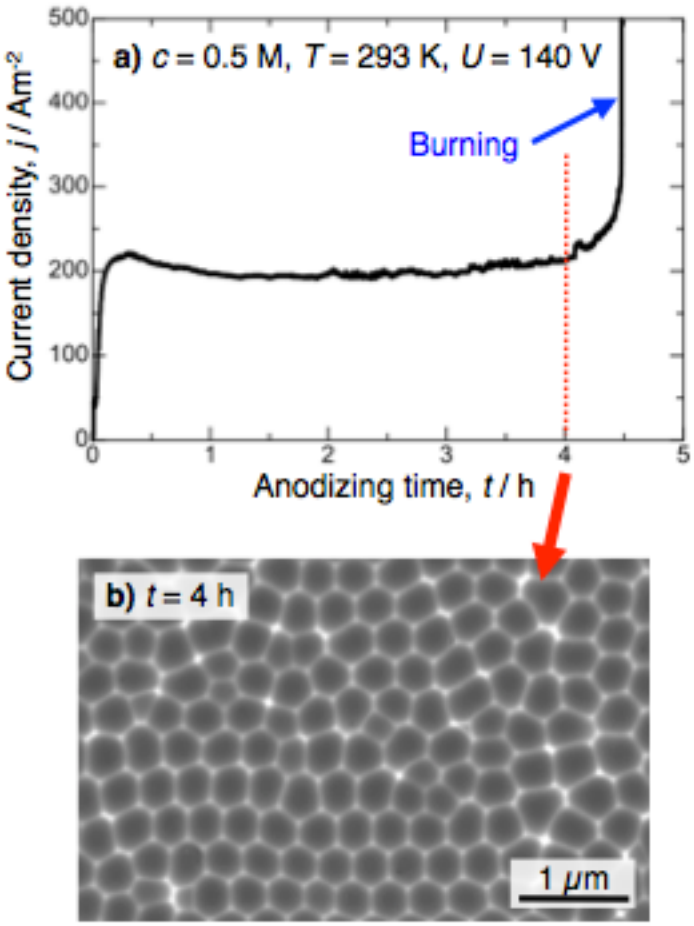
a) c = 0.5 M, T = 293 K, U = 140 V
Burning
Current density, j / Am-2
Anodizing time, t / h
b) t = 4 h
1 μm

Figure 8.

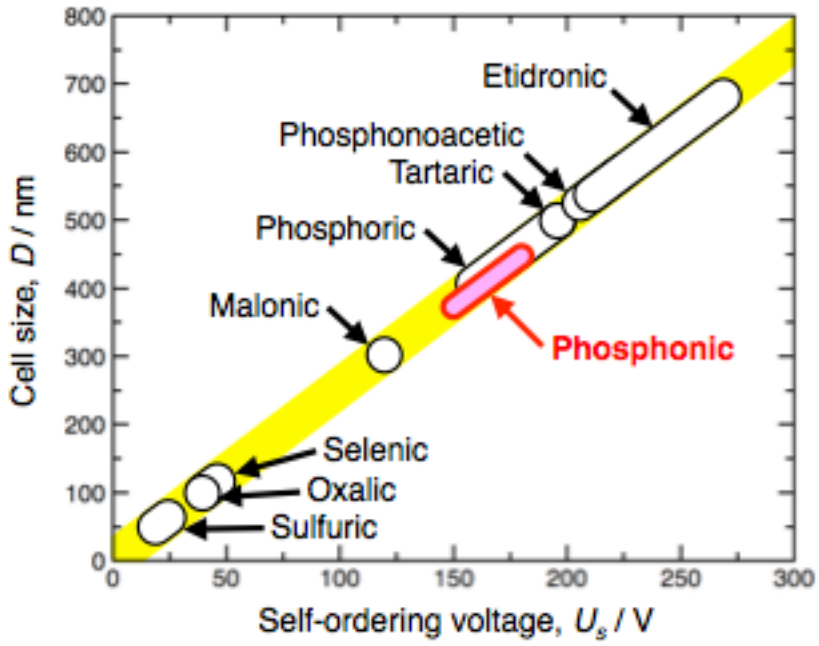
Cell size, D / nm
Self-ordering voltage, U_s / V
0
100
200
300
400
500
600
700
800
0
50
100
150
200
250
300
Etidronic
Phosphonoacetic
Tartaric
Phosphoric
Malonic
Phosphonic
Selenic
Oxalic
Sulfuric

Figure 9.

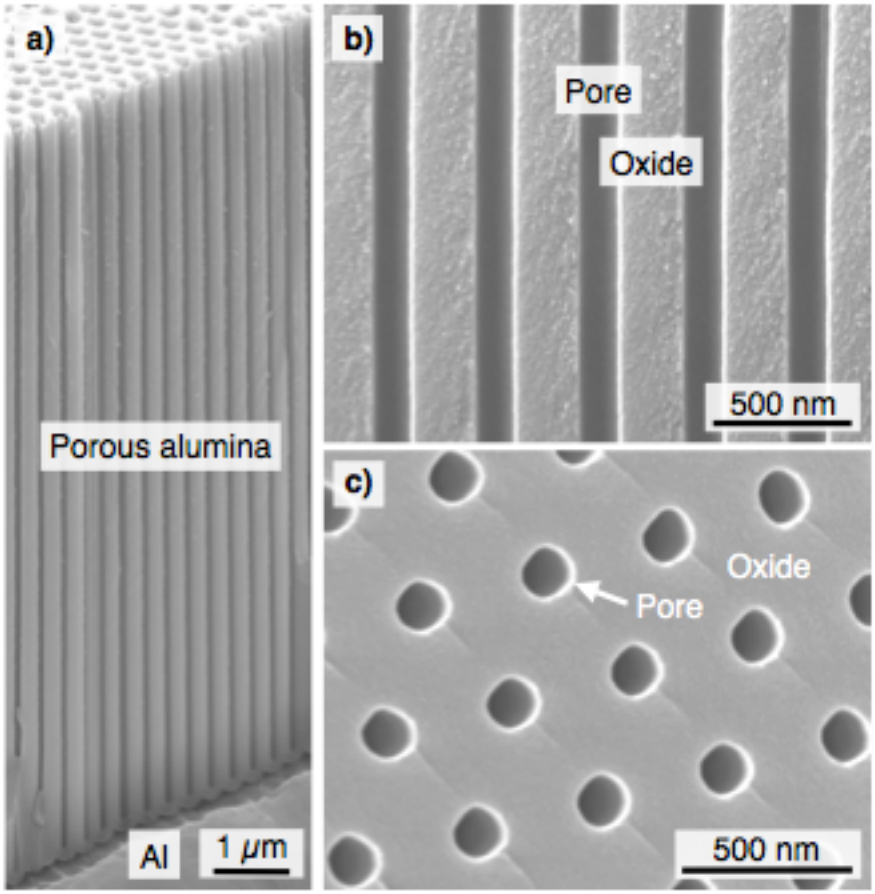

Figure 10.

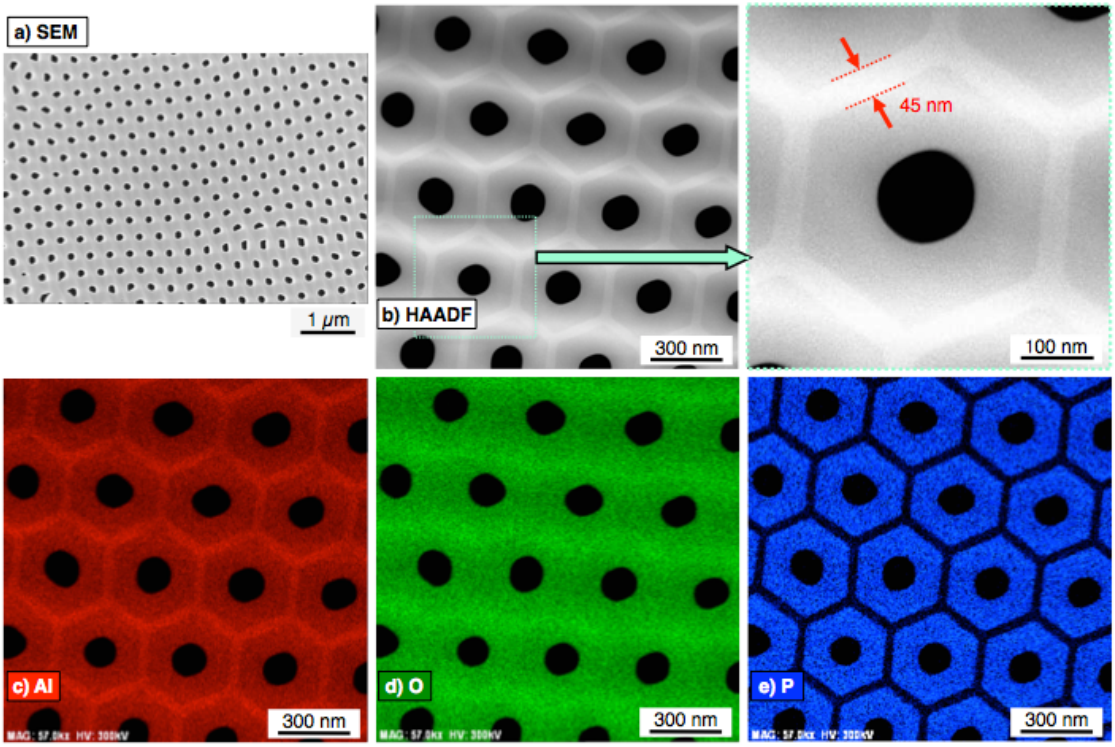

Figure 11.